J Paleolimnol (2014) 51:253–266
DOI 10.1007/s10933-013-9702-1

ORIGINAL PAPER

Monsoonal forcing of Holocene paleoenvironmental change on the central Tibetan Plateau inferred using a sediment record from Lake Nam Co (Xizang, China)

Stefan Doberschütz · Peter Frenzel · Torsten Haberzettl · Thomas Kasper · Junbo Wang · Liping Zhu · Gerhard Daut · Antje Schwalb · Roland Mäusbacher

Received: 23 January 2012 / Accepted: 26 February 2013 / Published online: 12 March 2013

Abstract This study focuses on Holocene monsoon dynamics on the central Tibetan Plateau (TP) inferred using a sediment record from Lake Nam Co. A high-resolution (decadal) multi-proxy approach, using geochemical, micropaleontological, and sedimentological methods was applied. Fifteen AMS-^{14}C ages were used to establish the chronology, assuming a reservoir effect of 1,420 years. Our results point to a first strong monsoonal pulse at Lake Nam Co ~11.3 cal ka BP, followed by colder and drier conditions until ~10.8 cal ka BP. A warm and humid climate from ~10.8 to ~9.5 cal ka BP is related to a strong summer monsoon on the central TP, triggering a lake-level highstand at ~9.5 cal ka BP. Declining minerogenic input after ~9.5 cal ka BP indicates less moisture availability until ~7.7 cal ka BP. Following stable conditions between ~7.7 and ~6.6 cal ka BP, a warm and wet climate is inferred for the time span from ~6.6 to ~4.8 cal ka BP. A change towards drier conditions after ~4.8 cal ka BP points to a weakening of the Indian Ocean Summer Monsoon on the central TP, further diminished after ~2.0 cal ka BP. A short-term wet spell occurred from ~1.5 to ~1.3 cal ka BP. By comparing the results derived from Lake Nam Co with several lacustrine records from the central, northern, and eastern TP, a similar but not synchronous pattern of monsoon-driven paleoenvironmental change is observed. Although the general trend of lake and catchment evolution on the TP during the Holocene is also reproduced in this record, pronounced spatial and temporal offsets with respect to distinct climate events were detected, suggesting periods of non-uniform moisture and temperature evolution.

Keywords Tibetan Plateau · Nam Co · Paleohydrology · Paleoclimate · Indian Ocean Summer Monsoon · Holocene

Electronic supplementary material The online version of this article (doi:10.1007/s10933-013-9702-1) contains supplementary material, which is available to authorized users.

S. Doberschütz (✉) · T. Haberzettl · T. Kasper · G. Daut · R. Mäusbacher
Institute of Geography, Physical Geography, Friedrich Schiller University Jena, Löbdergraben 32, 07743 Jena, Germany
e-mail: stefan.doberschuetz@web.de

P. Frenzel
Institute of Earth Sciences, Friedrich Schiller University Jena, Jena, Germany

J. Wang · L. Zhu
Key Laboratory of Tibetan Environment Changes and Land Surface Processes (TEL), Institute of Tibetan Plateau Research (ITP), Chinese Academy of Sciences, Beijing, China

A. Schwalb
Institute of Geosystems and Bioindication, Technical University Braunschweig, Braunschweig, Germany

Introduction

Multiple lacustrine records on the Tibetan Plateau (TP) have been used to reconstruct monsoon-forced paleoenvironmental changes during the late Quaternary (Herzschuh 2006; Mischke et al. 2008; Mügler et al. 2010; Wischnewski et al. 2011). Both sampling resolution and age control, however, show high variability (Shen et al. 2005; Herzschuh et al. 2006; Morrill et al. 2006; Zhu et al. 2009). Although the general pattern of climate evolution on the TP is reproduced in numerous studies, uncertainties exist regarding the occurrence, duration, and supra-regional significance of distinct climate oscillations. Whereas regional discrepancies of moisture evolution on the TP were reported by Wischnewski et al. (2011), synchronous behavior of Lake Nam Co on the central TP and the Hongyuan peat bog on the northeastern TP was proposed by Kasper et al. (2012) for the late Holocene. Moreover, some lacustrine records are discontinuous (Morrill et al. 2006; Zhu et al. 2009), complicating detailed comparison of paleoenvironmental evolution at different sites. Despite these limitations, monsoonal forcing of environmental change on the TP is suggested by several authors (Morrill et al. 2006; Wu et al. 2006; Kramer et al. 2010a, b), highlighting the need for a high-resolution, multi-proxy study on late Quaternary monsoon dynamics on the TP.

Several sediment cores were obtained at different water depths at Lake Nam Co. Hydro-acoustical (lake-bottom profiling), geochemical, biogeochemical, sedimentological, and micropaleontological analyses were conducted to reconstruct changing paleoenvironmental conditions dating back to ~8.9 cal ka BP (Li et al. 2008, 2009; Zhu et al. 2008, 2010a; Daut et al. 2010; Frenzel et al. 2010; Mügler et al. 2010; Wang et al. 2010a). Nevertheless, some problems arise in comparing these records, because reservoir effect dating corrections used different methods (Zhu et al. 2008; Mügler et al. 2010). In addition, distinct lake level changes are assumed to have resulted in depositional gaps within the cores because of reworking of material at the coring location during lower lake levels. Therefore, a continuous record of the entire Holocene derived from the deepest central part of Lake Nam Co is still missing.

For our study, sediments were recovered from the central part of the lake, providing a continuous lacustrine sediment record reaching beyond the LGM. Only the Holocene part of the core is discussed here. This study aims to reconstruct the Holocene evolution of the Indian Ocean Summer Monsoon (IOSM) on the central TP at multi-decadal (~50-year) resolution. Geochemical, sedimentological, and micropaleontological methods were used to identify high- and low-amplitude changes in sediment composition, indicating paleoenvironmental changes associated with strengthened or weakened monsoonal pulses (Wu et al. 2006; Zhu et al. 2008). The timing of these changes is used for comparison of monsoon-forced lake system responses on the central, northern, and eastern TP.

Study site

Lake Nam Co (30.7°N, 90.7°E, 4,718 m asl, Fig. 1a) is located in the south-central part of the TP. From W to E, the lake has a maximum length of ~78 km and a maximum N to S distance of ~44 km (Wang et al. 2010a). In 2004, a surface area of 2,015 km^2 was estimated (Zhu et al. 2010b). The maximum water depth is 98.9 m (Wang et al. 2009). As a high-mountain lake, Nam Co is covered by ice for 3–5 months per year. The pH of the water body ranges from 8.0 to 9.8 (Wang et al. 2009). Because Nam Co is a terminal lake, the water balance is primarily controlled by precipitation, evaporation, and freshwater supply from the catchment. The latter comprises an area of 10,600 km^2 (Zhang et al. 2008).

According to Liu (1998), the Nam Co region has a semi-arid subarctic plateau climate. For the time span from 14 July, 2005 to 13 July, 2006, a mean temperature of 0 °C was recorded. The annual precipitation is 282 mm for the given period, dominated by summer monsoon precipitation (You et al. 2006).

The Nam Co lake basin is of tectonic origin and was formed by uplift processes of the Himalayan Mountains during the Tertiary (Guan et al. 1984). Deposits near the lake shore are composed of unconsolidated Pleistocene to Holocene sediments of glacial, glaciofluvial, and fluvial origin. In addition, lacustrine and aeolian sediments occur within the catchment (Lehmkuhl et al. 2002).

Materials and methods

Prior to coring, hydro-acoustic profiling of the lake bottom was performed (Daut et al. 2010). Using a

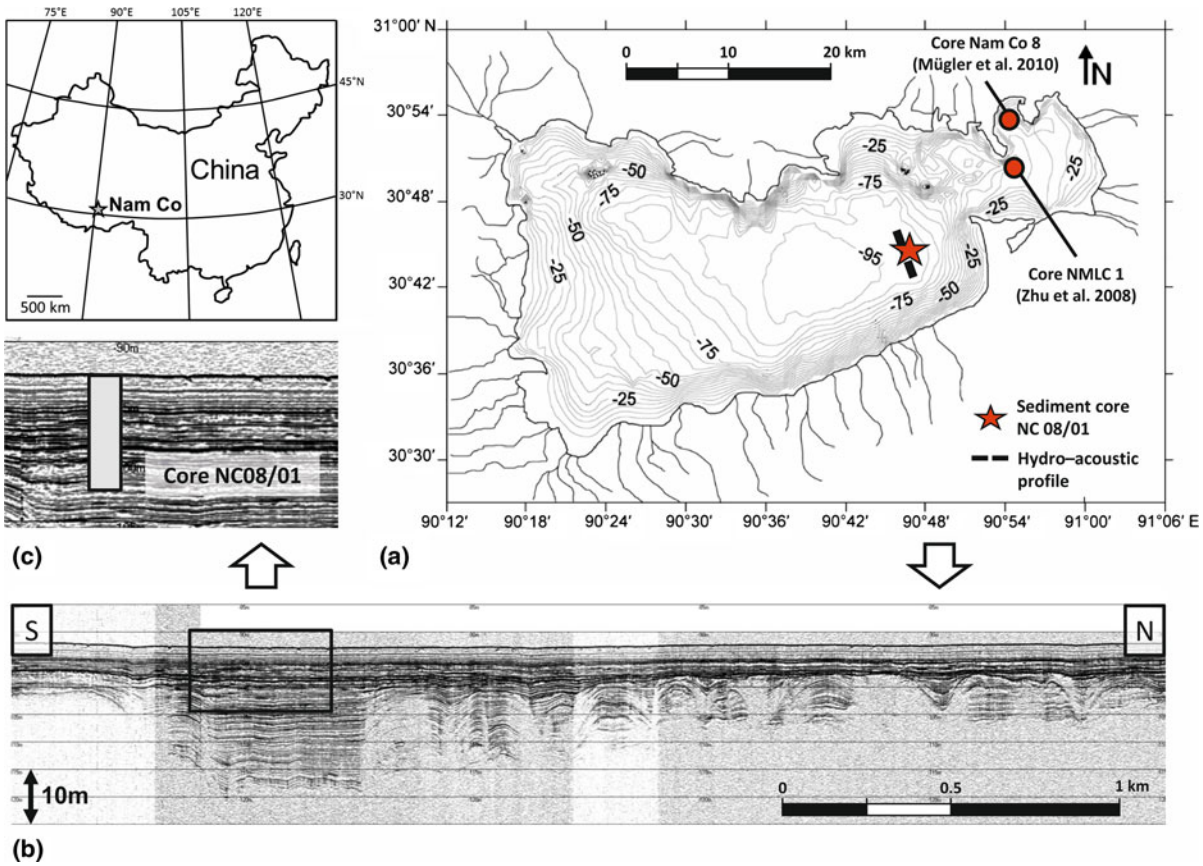

Fig. 1 Lake Nam Co on the central Tibetan Plateau (Xizang, China). The *line at the filled star marks* the track of the hydro-acoustic profile (**a**). The coring locations of sediment cores analyzed by Zhu et al. (2008) and Mügler et al. (2010) are indicated by *filled circles*. Sediment coring was performed in the southeast of Lake Nam Co, *highlighted* by the framed image section (**b**, **c**). Bathymetric map from Wang et al. (2009)

parametric echo sounding system (SES 96 light, Innomar Technologie GmbH), well-layered and undisturbed sediments ≥35 m thick (no basement) were detected in the SE of Lake Nam Co and selected for core retrieval (Fig. 1b, c).

Five gravity cores and one piston core (NC 08/01, 30.73°N, 90.78°E) were obtained at a water depth of 93 m using a modified gravity corer (ID 63 mm) (Meischner and Rumohr 1974) and an UWITEC piston corer (ID 90 mm). Using patterns of magnetic susceptibility, a composite record 10.4 m long was generated from gravity core NC 08/01 Pilot 3 and the piston core.

Laboratory methods

AMS-^{14}C dating of fifteen bulk sediment samples (Table 1) was performed by Beta Analytic. A reservoir effect of 1,420 years, obtained by dating surface sediment, was subtracted from all radiocarbon ages. Inverted ages at the top of the sequence from 26.5 to 6.5 cm sediment depth were omitted as outlined by Kasper et al. (2012), using ^{137}Cs and ^{210}Pb data. Corrected ages were calibrated with OxCal 4.1.7 (Bronk Ramsey 2009; Reimer et al. 2009). For establishing the chronology (Fig. 2), median values of calibrated ages were included in a deposition model (Bronk Ramsey 2008).

Grain size distributions at 1-cm resolution were obtained using a Microtrac S3500 Particle Size Analyzer. Samples were treated with hydrogen peroxide to remove organic matter. Carbonates were dissolved by hydrochloric acid. Grain sizes were condensed to classes of clay (<2 μm), silt (2–63 μm), and sand (63–2,000 μm). In addition, the median was calculated.

Table 1 ^{14}C-AMS ages for sediment core NC 08/01

Lab. no. (Beta Analytic)	Depth (cm)	AMS radiocarbon age (cal a BP)	Reservoir-corrected age (cal a BP)	2σ Calibration (Oxcal 4.1.7)	
				Median (cal a BP)	Error range (cal a BP)
260883	0.0	1,420 ± 40			
277415*	6.5	2,550 ± 40	1,130 ± 40	1,030	1,170–960
269540*	10.5	1,900 ± 40	480 ± 40	520	620–470
277416*	14.5	2,310 ± 40	890 ± 40	810	920–730
260884*	20.5	2,200 ± 40	780 ± 40	710	770–670
277417*	26.5	1,970 ± 40	550 ± 40	560	650–510
269541	35.5	1,930 ± 40	510 ± 40	530	630–500
277418	46.5	2,490 ± 40	1,070 ± 40	980	1,060–930
269542	65.5	2,910 ± 40	1,490 ± 40	1,370	1,520–1,300
260872	104.5	3,550 ± 40	2,130 ± 40	2,110	2,300–2,000
269537	134.5	4,540 ± 40	3,120 ± 40	3,350	3,440–3,250
269536	176.6	6,660 ± 40	5,240 ± 40	5,990	6,180–5,920
260873	206.6	9,060 ± 50	7,640 ± 50	8,440	8,540–8,380
269538	236.6	11,320 ± 60	9,900 ± 60	11,320	11,600–11,210
271057	278.2	12,060 ± 60	10,640 ± 60	12,590	12,700–12,430

Omitted ^{14}C-AMS ages (Kasper et al. 2012) are marked with an asterisk

Sediments were analyzed with an ITRAX XRF Core-Scanner (Cox Analytical Systems), producing multiple element scan profiles with a step size of 2 mm. Geochemical analyses were carried out applying ICP-OES (Varian Liberty 150, Agilent Technologies). In total, 237 samples were processed, applying a microwave-assisted, modified *aqua regia* digestion. In addition, an HCl digestion was performed for 113 samples (4-cm interval) to separate carbonate-bound and non-carbonate fractions of different elements. To ensure data reliability, a certified reference material (River sediment LGC6 187) was analyzed in the same way. Error estimates were based on triple measurements of individual samples, shown as error bars (Fig. 3).

Total carbon (TC), total organic carbon (TOC), total nitrogen (TN), and total sulfur (TS) were measured with a CNS elemental analyzer (Vario El, Elementar Analysensysteme GmbH). Total inorganic carbon (TIC) content was calculated by subtracting TOC from TC. Again, 237 samples were processed, covering the whole core section with a spatial resolution of ~1 cm. Triple measurements were carried out to quantify the analytical error (Fig. 3). TOC and TN were used to calculate atomic C/N ratios.

About 4 ml of sediment per sample were used for micropaleontological analysis. The sediment was disintegrated by wet-sieving (200-μm mesh size) and dried at room temperature. All ostracods were picked, checked for preservation and adult/juvenile ratio, and counted. Valves with evidence of transport or dissolution were excluded from counting as tentatively allochthonous. The ostracod accumulation rate was calculated using the sample-specific sedimentation rates derived from the chronology and a reference dry-weight of 1 g per sample. Because of frequently low ostracod numbers, up to five adjacent samples were grouped together to obtain at least 50 valves for calculating relative abundances within the ostracod association of every sample group. Where this number could not be reached, no relative abundances were calculated. Between ~5.7 and ~3.3 cal ka BP, no micropaleontological sampling was performed.

Results

The uppermost 2.5 m of the record comprise the Holocene. Accumulation rates ranging between 0.13 mm per year (~11.3 to ~3.3 cal ka BP) and 0.4 mm per year (since ~3.3 cal ka BP) were calculated (Fig. 2).

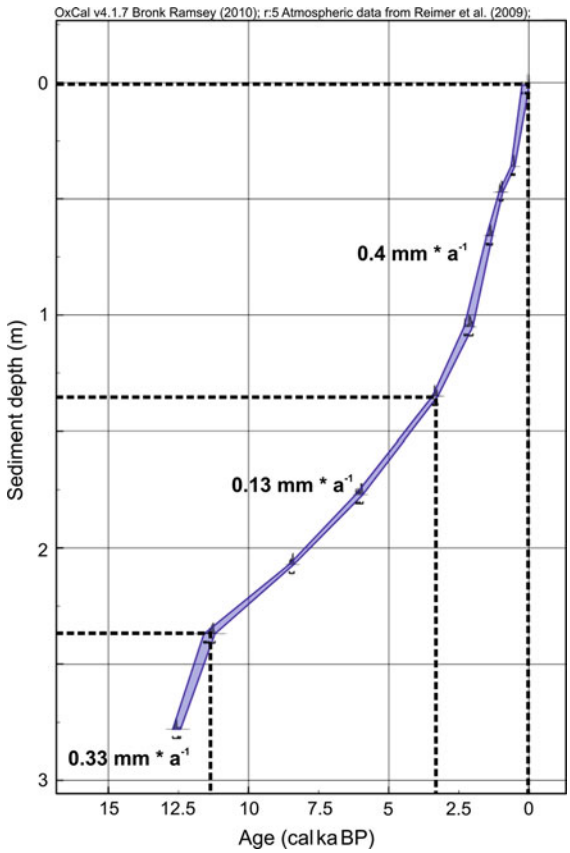

Fig. 2 Age-depth relationship and sediment accumulation rates for core NC 08/01. *Dashed lines* show periods of different mean annual lake sedimentation

Distinct changes in carbon, nitrogen, and sulphur are recorded between ~11.3 and ~7.7 cal ka BP, marked by a drop in TIC at ~11.3 cal ka BP, the Holocene minimum in TOC at ~11.2 cal ka BP, and a subsequent long-term, high-amplitude decrease in TIC, culminating at ~9.5 cal ka BP. The latter is accompanied by rising values of TOC, TN, and TS (Fig. 3). Subsequently, the reverse pattern is observed, showing a decrease in TOC, TN, and TS, especially after ~8.3 cal ka BP. During that time, an increase in TIC is recorded, reaching highest values from ~7.7 to ~6.6 cal ka BP (Fig. 3).

High-amplitude changes in major elements are centered at ~11.3 and ~9.5 cal ka BP, expressed by both a decline in Ca and Sr and a rise in K, Al, Rb, Ti, and Fe (Fig. 3). After ~9.5 cal ka BP, rising concentrations of Ca and Sr occur, with highest values from ~7.7 to ~6.6 cal ka BP. For K, Al, Rb, Ti, and Fe, a decrease is recorded until ~7.7 cal ka BP, followed by a slight increase after ~6.6 cal ka BP. From ~6.6 to ~2.0 cal ka BP, oscillations of lower amplitude are observed.

A distinct increase in Ca at ~2.0 cal ka BP is linked to a contemporaneous decrease in K, Al, Rb, Ti, and Fe. After ~0.25 cal ka BP, a diverse pattern is visible, marked by an increase in Ti, Rb, and Fe and a decline in Ca, K, and Al (Fig. 3). Mg shows a short-duration maximum at ~4.0 cal ka BP and rising concentrations after ~3.5 cal ka BP (Fig. 3). The Fe/Mn ratio displays rising values from ~10.9 to ~9.4 cal ka BP and small peaks at ~5.9 and ~4.0 cal ka BP (Fig. 3).

Grain-size distributions show low variability throughout the Holocene. Sediments are mainly composed of silt, with minor contributions of clay and sand (Fig. 3). The median of the grain sizes ranges from 4.0 to 18.1 µm, with an average median of 7.2 µm. A slight shift to finer material is displayed by the median at ~6.9 cal ka BP, showing a decline from 6.9 µm (~11.6 to ~6.9 cal ka BP) to 5.4 µm (~6.9 to ~2.0 cal ka BP). For the last ~2.0 cal ka BP the median increases to a mean value of 8.9 µm.

The ostracod record shows high valve accumulation rates from ~11.6 to ~10.8 cal ka BP (Fig. 3). The minimum in ostracod abundance between ~10.1 and ~8.9 cal ka BP is followed by a short-term increase ~8.0 cal ka BP and low accumulation rates from ~7.9 to ~5.7 cal ka BP. Increased abundance is recorded at ~3.3 cal ka BP. After ~3.3 cal ka BP distinct oscillations occur, showing the highest abundance at ~2.4 cal ka BP and two minima at ~0.6 and ~0.5 cal ka BP (Fig. 3). The ostracod associations show a rather monotonous species composition. The dominating species is *Leucocytherella sinensis* Huang, 1982, which makes up ≥50 % of the association in almost all samples (Fig. 1, Electronic Supplementary Material). ?*Leucocythere dorsotuberosa* Huang, 1982 is slightly more abundant after ~2.5 cal ka BP and reaches dominances similar to those of *Leucocytherella sinensis* after ~0.2 cal ka BP. *Fabaeformiscandona gyirongensis* Yang, 1982 is rare from ~11.6 to ~3.3 cal ka BP and is found in high proportions from ~2.5 to ~0.8 cal ka BP (Fig. 1, ESM). All other species are rare and show scattered occurrences, except for *Candona xizangensis* Huang, 1982, which is present in most samples, but in small numbers. *Candona candida* O. F. Müller, 1776, *Eucypris gyirongensis* Yang, 1982, and *Limnocythere inopinata*

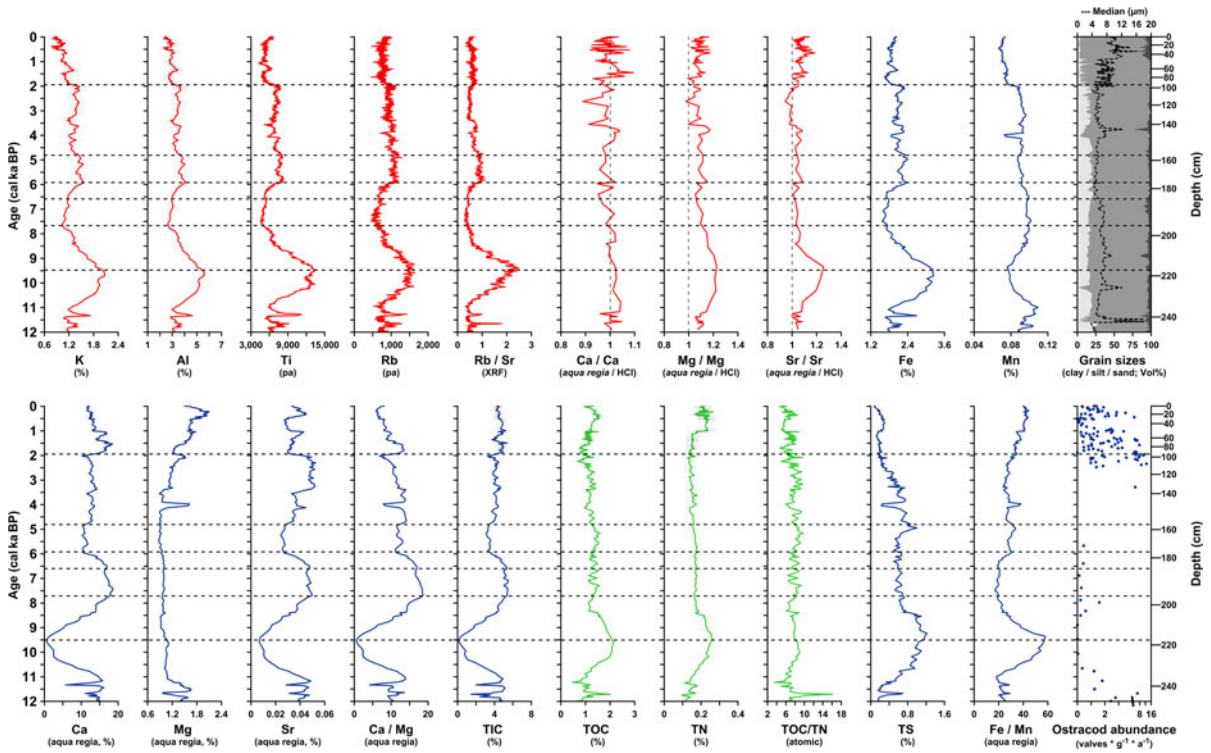

Fig. 3 Geochemical, sedimentological, and micropaleontological properties of the record. *Dashed lines* mark prominent time intervals of distinct changes mentioned in the text. The unit pa (peak area) refers to XRF-derived data. Note that no micropaleontological sampling was performed between ~5.7 and ~3.3 cal ka BP

Baird, 1843 are found more frequently from ~0.7 cal ka BP to present (Fig. 1, ESM).

Discussion

Lake productivity and autochthonous carbonate precipitation

Lake productivity in Lake Nam Co is assumed to be indicated by biologically precipitated carbonates and the amount of aquatic organic material. In addition, a chemical pathway of carbonate precipitation is taken into account, showing a strong linkage to productivity related processes, as both are primarily triggered by hydrological and hydrochemical variations and changing temperatures (Daut et al. 2010; Mügler et al. 2010). To assess the accumulation of carbonates, both Mg and Ca are used. Ca, highly correlated to TIC ($r = 0.93$), was chosen instead of TIC, which shows larger measurement uncertainty. High concentrations of Mg and Ca are supposed to show enrichment of carbonates as a consequence of intense biological or chemical precipitation (Daut et al. 2010).

Accumulation of organic matter is indicated by TOC, TN, and the TOC/TN ratio (Meyers and Ishiwatari 1993; Meyers 2003), of which TOC is linked to air and water temperatures (Zhu et al. 2008, 2010a). The nutrient supply is represented by TN (Meyers 2003). A high proportion of TOC points to enhanced autochthonous production or allochthonous influx of organic matter, which are further differentiated by the TOC/TN ratio (Mayr et al. 2005). Intense decomposition of organic material can result in anoxic conditions at the lake bottom, indicated by TS and rising levels of the Fe/Mn ratio (Tracey et al. 1996; Holmer and Storkholm 2001; Haberzettl et al. 2007).

The ostracod accumulation rate may indicate benthic productivity, reflecting changing reproduction rates of ostracods. Benthic productivity is linked to planktonic productivity and submersed macrophyte density. Thus, it is strongly influenced by water depth, with highest productivity in shallow water. Hence, higher ostracod accumulation rates suggest higher

lake productivity (Boomer et al. 2005). Other factors that influence the ostracod accumulation rate might include syndepositionary dissolution of the calcitic valves, transport processes, or oxygen deficiency at the lake bottom (Griffiths and Holmes 2000; Zhu et al. 2010a).

A clear linkage between lake productivity, as well as autochthonous carbonate precipitation, to variations in monsoon strength is suggested by this study. Changes in monsoonal precipitation, air temperatures, and associated glacier melt-water release should be recorded as both a hydrological signal, via varying carbonate precipitation, and a temperature signal (TOC accumulation) within the lake. A strengthening of the monsoon, and hence warm and wet conditions, might result in low autochthonous carbonate accumulation as a consequence of less chemical precipitation and a lack of benthic ostracods. Higher amounts of TOC can be linked to rising temperatures or slower degradation of organic material under anoxic conditions.

Reduced temperatures can be inferred from the drop in TOC between ~11.3 and ~11.2 cal ka BP. The lowering of Ca at ~11.3 cal ka BP and from ~11.2 to ~9.5 cal ka BP (Fig. 3) suggests a decline of carbonate accumulation or a lack of biota. Especially from ~10.9 to ~9.4 cal ka BP, the high Fe/Mn ratio indicates anoxic conditions at the lake bottom, probably responsible for the minimum of ostracod abundances documented between ~10.1 and ~8.9 cal ka BP, at low temporal sampling resolution. Because the preservation of valves is generally good and no dissolution evidence was observed, carbonate dissolution is excluded as a reason for the abundance minimum. Therefore, low Ca is believed to primarily indicate less chemical carbonate precipitation and a declining abundance of benthic ostracods. Rising concentrations of TOC, TN, and TS during these times of low Ca content can be explained by better preservation of organic material under anoxia, or may be linked to greater production of aquatic organic matter, as the low TOC/TN ratio (<10) suggests dominance of autochthonous material (Meyers 2003). The latter would indicate warmer conditions, especially at ~9.5 cal ka BP. As a consequence of this monsoon-forced warming, glaciers within the catchment would have released large amounts of freshwater, triggering lake expansion and causing less chemical as well as biological carbonate precipitation. The latter is probably caused by at least temporary oxygen deficiency at the lake bottom, diminishing benthic ostracods.

Increasing concentrations of Ca after ~9.5 cal ka BP are possibly related to a lowering of carbonate solubility caused by a rising salinity as a result of lake level decline. Hence, an intense chemical precipitation of carbonates under drier conditions, culminating between ~7.7 and ~6.6 cal ka BP, is inferred. Alternatively, a bloom of planktonic and benthic Ca-bearing organisms might be inferred, as indicated by the peak of the ostracod accumulation rate at ~8.0 cal ka BP. The latter is supported by the decline of TS, suggesting the development of a more oxygenated lake bottom environment. Declining values of TOC, TN, and TS during this period (~9.5 to ~6.6 cal ka BP) may indicate intense decomposition of organic material or less accumulation of organic material, suggesting colder conditions, especially at ~8.3 cal ka BP. From ~7.7 to ~6.6 cal ka BP, high levels of Ca accumulation probably driven by phytoplankton productivity or chemical precipitation are recorded, indicating drier conditions. The scarceness of ostracods during this period might point to lower annual temperatures or a stronger annual temperature gradient. Longer ice coverage can diminish oxygen availability, at least seasonally, at the lake bottom, resulting in low numbers of ostracods even under shallower-water conditions at the coring location.

The drop in Ca after ~6.6 cal ka BP (Fig. 3) indicates less carbonate precipitation. Benthic organisms are probably absent as a result of anoxia, as shown by rising Fe/Mn values at ~5.9 cal ka BP. TOC and TN suggest low variability of temperature and nutrient supply during that time.

A distinct peak of Mg at ~4.0 cal ka BP is probably related to an intense chemical precipitation of Mg-rich carbonates. Enhanced accumulation of carbonates is further accelerated after ~3.5 cal ka BP as shown by Ca and Mg ~2.0 and by Ca ~1.1 cal ka BP, showing drier conditions. An intense biological precipitation of carbonates is indicated by the high ostracod abundance at ~3.3 cal ka BP and after ~2.4 cal ka BP. A slight shift to less biological carbonate precipitation and probably lower temperatures is recorded for the last ~0.25 cal ka BP, as shown by the decreasing abundance of ostracods and the lowering of the TOC.

Allochthonous sediment influx

Bedrock weathering, glacial erosion, and periglacial processes are major sources of fine-grained debris within the catchment, which can be transported into the lake. Moreover, glacier melt water contributes a high proportion of suspended allochthonous sediments to the lake. For quantifying fluxes of clastic material, multiple elements, e.g. K, Al, Fe, Rb, and Ti have been used (Haberzettl et al. 2005, 2006; Wu et al. 2006; Daut et al. 2010). Elemental ratios of Ca/Ca, Mg/Mg, and Sr/Sr (*aqua regia*/HCl) are also applied as a proxy of allochthonous sediment input. A ratio of >1 is assumed to show non-carbonate phases of Ca, Mg, and Sr as part of the minerogenic input. The ratio of Rb and Sr was used to evaluate the sediment supply from the catchment. A positive shift of the Rb/Sr ratio is interpreted to indicate an increased influx of terrigenious material (Xu et al. 2010).

High concentrations of allochthonous elements point to enhanced moisture supply within the catchment. This is probably caused by intensified glacier melt water release, primarily triggered by changing temperatures, or an increase in precipitation. Both processes are directly controlled by the strength of the IOSM at Lake Nam Co by means of latent heat flux and moisture transport (Herzschuh 2006). Periods of strong monsoon intensity probably resulted in an intensified fluvial input of clastic material.

High-amplitude changes of sediment influx from ~11.3 to ~7.7 cal ka BP show enhanced levels of minerogenic input and wetter conditions at ~11.3 cal ka BP, a drier climate from ~11.2 to ~10.8 cal ka BP, and maximum moisture supply from ~10.0 to ~9.2 cal ka BP (Fig. 3). Centered at ~9.5 cal ka BP, elemental ratios of Ca, Mg, and Sr show an increased accumulation of allochthonous material, also denoted by the peak of the Rb/Sr ratio at ~9.4 cal ka BP (Fig. 3). Hence, the strongest intensification of the monsoon is inferred at ~9.5 cal ka BP, followed by drier conditions until ~7.7 cal ka BP and a rather stable system with lowest rates of allochthonous minerogenic input from ~7.7 to ~6.6 cal ka BP.

Enhancement of moisture availability is recorded between ~6.6 and ~4.8 cal ka BP. A decrease of sediment input occurs after ~4.8 cal ka BP, followed by stable conditions up to ~2.0 cal ka BP, a prominent dry spell at ~2.0 cal ka BP, and a subsequent increase in moisture supply between ~1.5 and ~1.3 cal ka BP. The latter is followed by less minerogenic input and drier conditions after ~1.3 cal ka BP. A small increase in sediment influx likely occurred after ~0.25 cal ka BP (Figs. 3, 4).

Lake level changes

Because of overall homogeneity in grain size distributions, except for the last ~2.0 cal ka BP, changing lake levels are inferred from geochemical and micropaleontological proxies. Lower carbonate accumulation is believed to indicate expanding water volume as was observed in previous studies (Haberzettl et al. 2009). The abundance of ostracods is also coupled to water depth, showing the highest abundance in shallow waters. In addition, high levels of allochthonous elements suggest enhanced fluvial runoff. Therefore, these proxies denote lake level change, with rising lake levels linked to a strong IOSM.

High ostracod abundances and intense accumulation of carbonates indicate low lake level from ~11.6 to ~10.8 cal ka BP (Fig. 3), interrupted by a short-term lake level rise at ~11.3 cal ka BP. From ~10.8 to ~9.5 cal ka BP all proxies point to lake volume expansion. A lake level highstand is reached at ~9.5 cal ka BP, reflecting the Holocene optimum of moisture availability. A lowering of the lake level is inferred from ~9.5 to ~7.7 cal ka BP, probably tracing a transition from warm-humid to cold-dry conditions. A low lake level at ~8.0 cal ka BP is supported by the presence of shallow-water ostracods *Eucypris gyirongensis* and *Candona candida* (Fig. 1, ESM; Wrozyna et al. 2009; Frenzel et al. 2010). From ~7.7 to ~6.6 cal ka BP stable lake level is inferred.

Changes in both carbonate precipitation and minerogenic influx indicate lake level rise from ~6.6 to ~4.8 cal ka BP (Figs. 3, 4). This is supported by the slight fining of the sediments after ~6.9 cal ka BP (Fig. 3), pointing to a longer-distance transport of material to the coring location (Haberzettl et al. 2010) as a result of higher lake level. Decreasing lake level at ~4.0 and ~3.5 cal ka BP is recorded by enhanced accumulation of Mg-rich carbonates.

Amplified lake shrinkage occurs after ~2.0 cal ka BP. This period is followed by rising lake levels from ~1.5 to ~1.3 cal ka BP and lowering of the lake level at ~1.1 cal ka BP. The lake level decrease after ~0.7 cal ka BP is recorded by the shallow-water ostracods *Eucypris gyirongensis* and *Limnocythere*

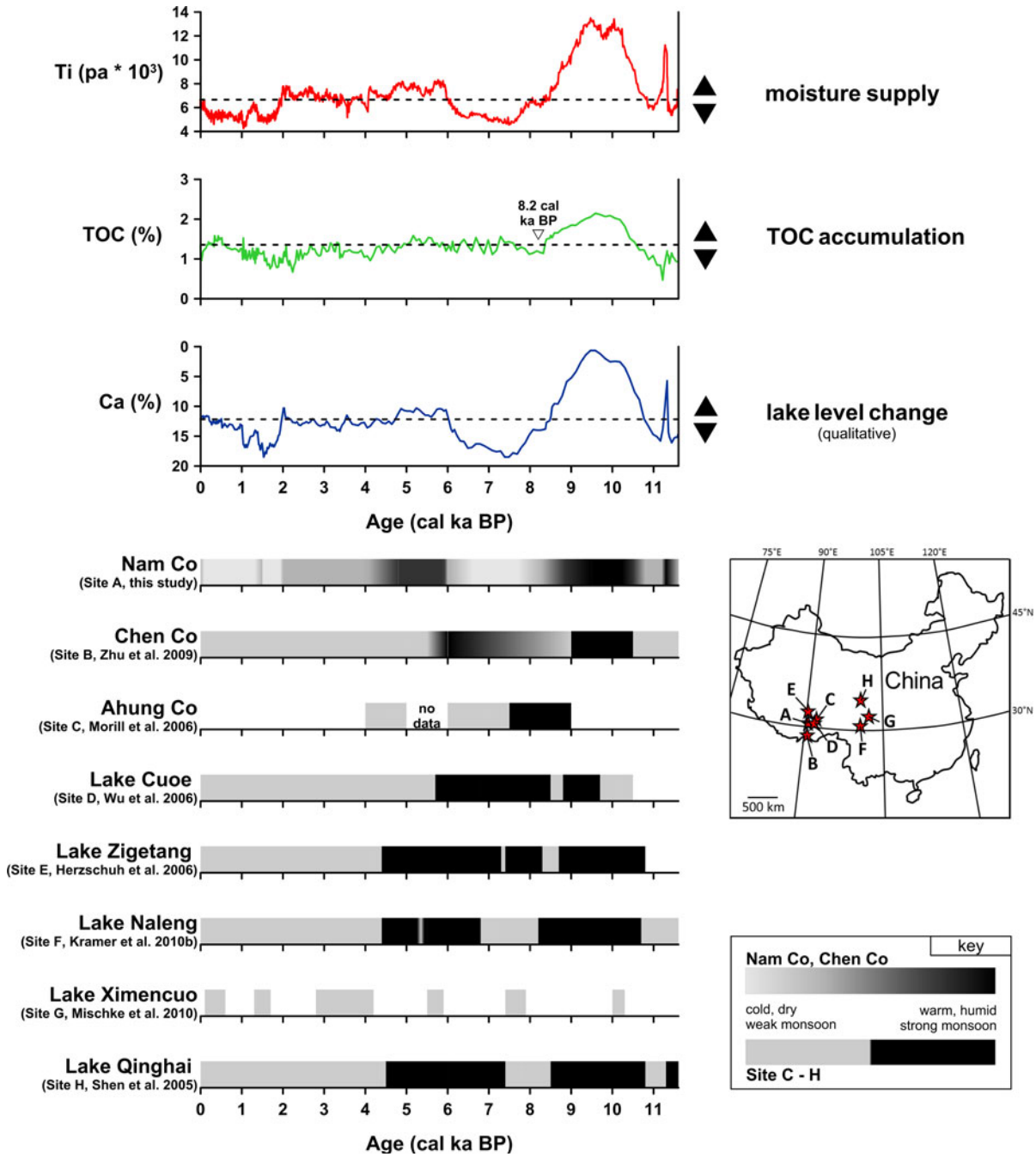

Fig. 4 Reconstruction of Holocene monsoon dynamics on the central, northern, and eastern Tibetan Plateau. *Broken lines* show elemental concentrations of Ti, TOC, and Ca derived from surface samples. The unit pa (peak area) refers to XRF-derived data. Note that an inverse scale is applied for Ca. For Lake Nam Co, a high-resolution and differentiated analysis of variations in monsoon strength was achieved, showing gradual changes on long and short time scales. For Lake Chen Co, a gradient color scheme is applied for the inferred transition from dry to wet conditions from 9.0 to 6.0 cal ka BP with no differentiations in between. At Lake Ximencuo, only cold events were discussed by Mischke and Zhang (2010). Note that a termination of lake sedimentation after 4.0 cal ka BP was recorded at Lake Ahung Co (Morrill et al. 2006)

inopinata (Wrozyna et al. 2009; Frenzel et al. 2010; Fig. 1, ESM). From ~0.25 cal ka BP to recent times, rising lake level is indicated by an increase in minerogenic input.

Monsoon-driven paleoenvironmental change on the central, northern, and eastern TP

Numerous lacustrine records from the central, northern, and eastern part of the TP show a consistent pattern of paleoenvironmental change during the Holocene. This is attributed to synchronous variations in the strength of the IOSM influencing these areas (Herzschuh 2006; Wang et al. 2010b; Zhang et al. 2011). For this study, a comparison of Lake Nam Co to adjacent lakes (Lakes Ahung Co, Chen Co, Cuoe, and Zigetang) as well as to large Lake Qinghai and small Lakes Naleng and Ximencuo, from the northern and eastern TP was conducted (Fig. 4). Lakes Chen Co, Nam Co, Cuoe, Ahung Co, and Zigetang span a S–N transect of approximately ~350 km on the central TP and may track spatial variations of moisture availability and temperature evolution as related to the strength of the IOSM. Lake Qinghai was used for a comparison to Lake Nam Co because of its comparable dimension. Lakes Naleng and Ximencuo are situated at the eastern limit of the IOSM (Kramer et al. 2010a, b; Mischke and Zhang 2010). Hence, both lakes, along with Lake Qinghai, are applied to reconstruct supra-regional patterns of monsoon-forced lake and catchment evolution on the TP. The lakes were also chosen because of their sampling resolution and age control. The records from Lakes Ahung Co, Naleng, and Ximencuo have high temporal resolution comparable to our record.

Wetter conditions at ~11.3 cal ka BP at Lake Nam Co provide the first evidence of an early Holocene intensification of the IOSM on the central TP, which has not been reported from other small and shallow lakes adjacent to Lake Nam Co. Humid conditions were also reported from the northeastern TP at Lake Qinghai from 12.3 to 11.3 cal ka BP (Fig. 4; Shen et al. 2005). This response on the central and northeastern TP suggests a supra-regional strengthening of the IOSM.

A dry and cold period from ~11.2 to ~10.8 cal ka BP at Lake Nam Co is linked to a cold and arid climate at Lake Qinghai from 11.3 to 10.8 cal ka BP (Shen et al. 2005), indicating a short-term phase of weakened monsoon at both sites (Fig. 4).

The high-amplitude shift to warmer and wetter conditions from ~10.8 to ~9.5 cal ka BP is also observed in several lacustrine records, showing a warm and humid climate after 11.1 cal ka BP (Lake Ximencuo, Mischke and Zhang 2010), 10.8 cal ka BP (Lake Zigetang, Herzschuh et al. 2006; Lake Qinghai, Shen et al. 2005), 10.7 cal ka BP (Lake Naleng, Kramer et al. 2010a, b), 10.5 cal ka BP (Lake Chen Co, Zhu et al. 2009), and 9.7 cal ka BP (Lake Cuoe, Wu et al. 2006). Hence, all lake records seem to confirm an almost synchronous supra-regional increase in summer monsoon intensity during the early Holocene (Fig. 4). The temporal offset at Lake Cuoe was probably caused by catchment processes and a transition from a fluvial to a lacustrine sedimentary environment at 10.1 cal ka BP (Wu et al. 2006).

The lower lake levels, attributed to a continuous shift to drier conditions and weaker monsoon intensity at Lake Nam Co from ~9.5 to ~7.7 cal ka BP (Fig. 4), confirm previous results on less moisture supply at Lake Nam Co for the period from 8.1 to 7.8 cal ka BP (Zhu et al. 2008). The drop in TOC after ~8.3 cal ka BP (Fig. 4) is possibly related to the 8.2 ka cold event, detectable in oxygen isotope data from the GRIP ice core (Andersen et al. 2007). A prominent cold and dry period after 9.0 cal ka BP at Lake Chen Co (Zhu et al. 2009), 8.8 cal ka BP at Lake Cuoe (Wu et al. 2006), 8.7 cal ka BP at Lake Zigetang (Herzschuh et al. 2006), 8.5 cal ka BP at Lake Qinghai (Shen et al. 2005), 8.1 cal ka BP at Lake Naleng (Kramer et al. 2010a, b), and 7.9 cal ka BP at Lake Ximencuo (Mischke and Zhang 2010) points to the occurrence of discrete time intervals (<1,000 a) of reduced moisture availability and lower temperatures on the central, northern, and eastern TP (Fig. 4). In contrast, our study suggests a continuous increase in aridity during the entire period from ~9.5 to ~7.7 cal ka BP.

Low-amplitude responses of Lake Nam Co to monsoonal pulses from ~7.7 cal ka BP to present are attributed to lower intensity in paleoenvironmental change or lower sensitivity of the lake. Our inferences of dry and probably cold conditions from ~7.7 to ~6.6 cal ka BP are supported by similar observations at Lake Naleng (8.1–7.2 cal ka BP, Kramer et al. 2010a, b), Lake Ximencuo (7.9–7.4 cal ka BP, Mischke and Zhang 2010), and Lake Ahung Co

(7.5–7.0 cal ka BP, Morrill et al. 2006). At Lake Zigetang, a cold event was recorded at 7.4 cal ka BP (Herzschuh et al. 2006). At Lake Qinghai, a drop in lake level occurred at 7.2 cal ka BP (Lister et al. 1991). Still wet, but colder conditions were documented for Lake Cuoe at 6.8 cal ka BP (Wu et al. 2006), also indicating a nonuniform pattern of cooler conditions and lower moisture availability at different sites (Fig. 4). Hence, these cold and dry spells seem to vary in space and time.

Humid conditions and strengthening of the IOSM at Lake Nam Co from ~6.6 to ~4.8 cal ka BP were also suggested by Zhu et al. (2008) based on a much coarser-temporal-resolution study reporting a warm and wet climate at 6.9 cal ka BP. In addition, high lake levels and pronounced minerogenic input at Lake Nam Co were also observed by Mügler et al. (2010). Although wet conditions were reported by Mügler et al. (2010) from 7.2 to 5.4 cal ka BP, geochemical data suggest an increase in moisture availability did not occur until 6.8 cal ka BP. Higher temperatures and considerably wetter conditions are also reported for Lake Zigetang (7.3–4.4 cal ka BP, Herzschuh et al. 2006), Lake Cuoe (6.8–5.7 cal ka BP, Wu et al. 2006), and Lake Chen Co (6.0 cal ka BP, Zhu et al. 2009), supporting our inference for wetter conditions on the central TP (Fig. 4). For Lake Qinghai, a warm and wet climate was inferred from 7.4 to 6.5 cal ka BP, followed by cooler and drier, but still humid conditions from 6.5 to 4.5 cal ka BP (Shen et al. 2005). In contrast, Lister et al. (1991) suggest lake level decrease from 7.2 to 6.8 cal ka BP and rising lake levels afterwards. Because the record from Lake Naleng (Kramer et al. 2010a, b) displays the same trend towards warm and humid conditions from 6.8 to 4.4 cal ka BP, an almost synchronous supra-regional strengthening of the IOSM during the mid Holocene is inferred (Fig. 4).

A further weakening of the IOSM at Lake Nam Co is dated to ~4.8 cal ka BP, delimiting warm and wet conditions until ~4.8 cal ka BP and a drier climate from ~4.8 to ~2.0 cal ka BP in a more precise way than Mügler et al. (2010), who simply report a change from stable lake levels at 5.4 cal ka BP to lower levels at 4.0 cal ka BP. According to their geochemical data, a distinct decrease in allochthonous influx occurs at around 4.9 cal ka BP, pointing to an increase in aridity at Lake Nam Co. The transition to drier conditions is supported by observations from Lakes Chen Co and Ahung Co, showing a dry and cold event at 4.8 cal ka BP at Lake Chen Co (Zhu et al. 2009) and less monsoonal precipitation at Lake Ahung Co after 4.7 cal ka BP (Morrill et al. 2006). A cold event occurs at Lake Cuoe after 4.6 cal ka BP (Wu et al. 2006). Cool conditions were reported for Lake Qinghai after 4.5 cal ka BP (Shen et al. 2005) and for Lake Naleng after 4.4 cal ka BP (Kramer et al. 2010a, b), suggesting an almost synchronous behavior of different lake systems to lower temperatures and reduced moisture availability (Fig. 4).

Higher evaporation at Lake Nam Co at ~4.0 cal ka BP (Figs. 3, 4) is inferred to have triggered a short-term lake level decrease, also proposed by Mügler et al. (2010) for a longer time span. A cold and dry event was inferred from both Lake Cuoe between 4.6 and 4.2 cal ka BP (Wu et al. 2006) and Lake Zigetang between 4.1 and 3.5 cal ka BP (Herzschuh et al. 2006). Less monsoonal precipitation at Lake Ahung Co caused a lake level low stand, resulting in a termination of sediment accumulation after 4.0 cal ka BP (Morrill et al. 2006). These dry and cold spells on the central TP are probably linked to increased aridity on the northern and eastern TP, recorded for significantly longer periods at Lake Qinghai (4.5–2.5 cal ka BP, Shen et al. 2005), Lake Naleng (4.4 cal ka BP to present, Kramer et al. 2010a, b), and Lake Ximencuo (4.2–2.8 cal ka BP, Mischke and Zhang 2010; Fig. 4). Therefore, non-uniform response of different lake systems to a weakened IOSM is suggested for the period from ~4.8 to ~2.0 cal ka BP.

A major shift towards drier conditions after ~2.0 cal ka BP is supported by findings of Mügler et al. (2010) and Kasper et al. (2012). A distinct decrease in precipitation at Lake Nam Co suggested by Zhu et al. (2008) for the period after 2.9 cal ka BP can also be linked to the ~2.0 cal ka BP dry spell in our record (Kasper et al. 2012). At Lake Qinghai, cold-arid conditions at 2.5 cal ka BP (Shen et al. 2005) indicate a weakened monsoon also on the northeastern TP.

The short-term wet spell from ~1.5 to ~1.3 cal ka BP at Lake Nam Co was not detected by Mügler et al. (2010), who inferred a dry climate from 1.6 to 1.4 cal ka BP and humid conditions from 1.4 to 0.8 cal ka BP. Nevertheless, our record indicates enhanced summer monsoon precipitation on the central TP for about 200 years (Fig. 4), also deduced from the Hongyuan peat bog on the northeastern TP from 1.5 to 1.2 cal ka BP (Hong et al. 2003). Because

no other lacustrine archives on the central, northern, and eastern TP document this oscillation, further research regarding this short-term wet spell is necessary.

Wetter conditions after ~0.25 cal ka BP suggest a strengthening of the IOSM on the central TP up to present. Satellite imagery and hydrological modelling indicate rising lake level for Lake Nam Co over the last few decades (Krause et al. 2010; Zhu et al. 2010b), confirming our inferences from sedimentary proxies for lake level.

Conclusions

The pattern of Holocene paleoenvironmental change at Lake Nam Co points to both long-term and short-term variations in moisture supply. Strong monsoonal pulses are inferred for the early Holocene at ~11.3 cal ka BP and from ~10.8 to ~9.5 cal ka BP, followed by a constant decrease of moisture availability up to ~7.7 cal ka BP. Rather stable conditions from ~7.7 to ~6.6 cal ka BP and a warm and wet climate from ~6.6 to ~4.8 cal ka BP point to a strong IOSM during the mid Holocene. Stepwise weakening of the monsoon is recorded at ~4.8 and ~2.0 cal ka BP, suggesting drier conditions at Lake Nam Co during the late Holocene.

Our assessment suggests a complex pattern of monsoon-forced moisture and temperature evolution on the central, northern, and eastern TP during the entire Holocene. Although the general trend of lake system responses seems to indicate a similar evolution at different sites, pronounced spatial and temporal offsets for some climate events were detected. It is unclear whether differences in sampling resolution, age control, regionally confined heterogeneities or selection of proxies (pollen, geochemical data, etc.) are responsible for the differences, or if they mask a rather uniform behavior of large and small lakes. Alternatively, asynchronous response of different lakes may indeed have occurred during certain time spans, highlighting the need for further research on this topic.

Acknowledgments This work is a contribution to the DFG priority program 1372 "Tibetan Plateau: Formation—Climate—Ecosystems (TiP)" grant no. MA1308/23-1. Additional funding was provided by the NSFC project (grant no. 41130529). We thank Brunhilde Dressler, Carmen Kirchner, Kati Hartwig, Rita Hempel, Frank Raphael, Stephanie Meschner, and Jifeng Zhang for geochemical, sedimentological, and micropaleontological analyses. Volker Wennrich and Armine Shahnazarian are acknowledged for supporting XRF analyses at the University of Cologne, Germany. Thanks to Marieke Ahlborn, Steffen Mischke, Mark Brenner and two anonymous reviewers for critical comments and discussions. We thank Richard Niederreiter (Uwitec, Austria) and our Chinese colleagues for their assistance during the field campaign in 2008.

References

Andersen KK, Bigler M, Buchardt SL, Clausen HB, Dahl-Jensen D, Davies SM, Fischer H, Goto-Azuma K, Hansson ME, Heinemeier J, Johnsen SJ, Larsen LB, Muscheler R, Olsen GJ, Rasmussen SO, Röthlisberger R, Ruth U, Seierstad IK, Siggaard-Andersen M-L, Steffensen JP, Svensson AM, Vinther BM (2007) Greenland ice core chronology 2005 (GICC05) and 20 year means of oxygen isotope data from ice core GRIP. doi:10.1594/PANGAEA.586836

Boomer I, von Grafenstein U, Guichard F, Bieda S (2005) Modern and Holocene sublittoral ostracod assemblages (Crustacea) from the Caspian Sea: a unique brackish, deep-water environment. Palaeogeogr Palaeoclimatol Palaeoecol 225:173–186

Bronk Ramsey C (2008) Deposition models for chronological records. Quat Sci Rev 27:42–60

Bronk Ramsey C (2009) Bayesian analysis of radiocarbon dates. Radiocarbon 51:337–360

Daut G, Mäusbacher R, Baade J, Gleixner G, Kroemer E, Mügler I, Wallner J, Wang J, Zhu L (2010) Late Quaternary hydrological changes inferred from lake level fluctuations of Nam Co (Tibetan Plateau, China). Quat Int 218:86–93

Frenzel P, Wrozyna C, Xie M, Zhu L, Schwalb A (2010) Palaeowater depth estimation for a 600-year record from Nam Co (Tibet) using an ostracod-based transfer function. Quat Int 218:157–165

Griffiths HI, Holmes JA (2000) Non-marine ostracods and Quaternary palaeoenvironments. Quaternary Research Association, London

Guan ZH, Chen CY, Ou YX, Fan YQ, Zhang YS, Chen ZM, Bao SH, Zu YT, He XW, Zhang MT (1984) Rivers and lakes in Tibet. Science Press, Beijing In Chinese

Haberzettl T, Fey M, Lücke A, Maidana N, Mayr C, Ohlendorf C, Schäbitz F, Schleser GH, Wille M, Zolitschka B (2005) Climatically induced lake level changes during the last two millennia as reflected in sediments of Laguna Potrok Aike, southern Patagonia (Santa Cruz, Argentina). J Paleolimnol 33:283–302

Haberzettl T, Wille M, Fey M, Janssen S, Lücke A, Mayr C, Ohlendorf C, Schäbitz F, Schleser GH, Zolitschka B (2006) Environmental change and fire history of southern Patagonia (Argentina) during the last five centuries. Quat Int 158:72–82

Haberzettl T, Corbella H, Fey M, Janssen S, Lücke A, Mayr C, Ohlendorf C, Schäbitz F, Schleser GH, Wille M, Wulf S, Zolitschka B (2007) Lateglacial and Holocene wet–dry cycles in southern Patagonia: chronology, sedimentology and geochemistry of a lacustrine record from Laguna Potrok Aike, Argentina. The Holocene 17:297–310

Haberzettl T, Anselmetti FS, Bowen SW, Fey M, Mayr C, Zolitschka B, Ariztegui D, Mauz B, Ohlendorf C, Kastner S, Lücke A, Schäbitz F, Wille M (2009) Late Pleistocene dust deposition in the Patagonian steppe-extending and refining the paleoenvironmental and tephrochronological record from Laguna Potrok Aike back to 55 ka. Quat Sci Rev 28:2927–2939

Haberzettl T, St-Onge G, Lajeunesse P (2010) Multi-proxy records of environmental changes in Hudson Bay and Strait since the final outburst flood of Lake Agassiz-Ojibway. Mar Geol 271:93–105

Herzschuh U (2006) Palaeo-moisture evolution in monsoonal Central Asia during the last 50,000 years. Quat Sci Rev 25:163–178

Herzschuh U, Winter K, Wünnemann B, Li S (2006) A general cooling trend on the central Tibetan Plateau throughout the Holocene recorded by the Lake Zigetang pollen spectra. Quat Int 154–155:113–121

Holmer M, Storkholm P (2001) Sulphate reduction and sulphur cycling in lake sediments: a review. Freshw Biol 46:431–451

Hong YT, Hong B, Lin QH, Zhu YX, Shibata Y, Hirota M, Uchida M, Leng XT, Jiang HB, Xu H, Wang H, Yi L (2003) Correlation between Indian Ocean summer monsoon and North Atlantic climate during the Holocene. Earth Planet Sci Lett 211:371–380

Kasper T, Haberzettl T, Doberschütz S, Daut G, Wang J, Zhu L, Nowaczyk N, Mäusbacher R (2012) Indian ocean summer monsoon (IOSM)-dynamics within the past 4 ka recorded in the sediments of Lake Nam Co, central Tibetan Plateau (China). Quat Sci Rev 39:73–85

Kramer A, Herzschuh U, Mischke S, Zhang C (2010a) Holocene treeline shifts and monsoon variability in the Hengduan Mountains (southeastern Tibetan Plateau), implications from palynological investigations. Palaeogeogr Palaeoclimatol Palaeoecol 286:23–41

Kramer A, Herzschuh U, Mischke S, Zhang C (2010b) Late Quaternary environmental history of the south-eastern Tibetan Plateau inferred from the Lake Naleng non-pollen palynomorph record. Veg Hist Archaeobot 19:453–468

Krause P, Biskop S, Helmschrot J, Flügel WA, Kang S, Gao T (2010) Hydrological system analysis and modelling of the Nam Co basin in Tibet. Adv Geosci 27:29–36

Lehmkuhl F, Klinge M, Lang A (2002) Late Quaternary glacier advances, lake level fluctuations and aeolian sedimentation in Southern Tibet. Z Geomorphol 126:183–218

Li M, Kang S, Zhu L, You Q, Zhang Q, Wang J (2008) Mineralogy and geochemistry of the Holocene lacustrine sediments in Nam Co, Tibet. Quat Int 187:105–116

Li M, Kang S, Zhu L, Wang F, Wang J, Yi C, Fang X, Xie M (2009) On the unusual Holocene carbonate sediment in Lake Nam Co, central Tibet. J Mt Sci 6:346–353

Lister GS, Kelts K, Zao CK, Yu J-Q, Niessen F (1991) Lake Qinghai, China: closed-basin lake levels and the oxygen isotope record for ostracoda since the latest Pleistocene. Palaeogeogr Palaeoclimatol Palaeoecol 84:141–162

Liu MG (1998) Atlas of physical geography. China Map Press, Beijing, China In Chinese

Mayr C, Fey M, Haberzettl T, Janssen S, Lücke A, Maidana NI, Ohlendorf C, Schäbitz F, Schleser GH, Struck U, Wille M, Zolitschka B (2005) Palaeoenvironmental changes in southern Patagonia during the last millennium recorded in lake sediments from Laguna Azul (Argentina). Palaeogeogr Palaeoclimatol Palaeoecol 228:203–227

Meischner D, Rumohr J (1974) A light-weight, high-momentum gravity corer for subaqueous sediments. Senckenb Marit 6:12

Meyers PA (2003) Applications of organic geochemistry to paleolimnological reconstructions: a summary of examples from the Laurentian Great Lakes. Org Geochem 34:261–289

Meyers PA, Ishiwatari R (1993) Lacustrine organic geochemistry—an overview of indicators of organic matter sources and diagenesis in lake sediments. Org Geochem 20:867–900

Mischke S, Zhang C (2010) Holocene cold events on the Tibetan Plateau. Glob Planet Change 72:155–163

Mischke S, Kramer M, Zhang C, Shang H, Herzschuh U, Erzinger J (2008) Reduced early Holocene moisture availability in the Bayan Har Mountains, northeastern Tibetan Plateau, inferred from a multi-proxy lake record. Palaeogeogr Palaeoclimatol Palaeoecol 267:59–76

Morrill C, Overpeck JT, Cole JE, Liu KB, Shen C, Tang L (2006) Holocene variations in the Asian monsoon inferred from the geochemistry of lake sediments in central Tibet. Quat Res 65:232–243

Mügler I, Gleixner G, Günther F, Mäusbacher R, Daut G, Schütt B, Berking J, Schwalb A, Schwark L, Xu B, Yao T, Zhu L, Yi C (2010) A multi-proxy approach to reconstruct hydrological changes and Holocene climate development of Nam Co, Central Tibet. J Paleolimnol 43:625–648

Reimer PJ, Baillie MGL, Bard E, Bayliss A, Beck JW, Blackwell PG, Bronk Ramsey C, Buck CE, Burr GS, Edwards RL, Friedrich M, Grootes PM, Guilderson TP, Hajdas I, Heaton TJ, Hogg AG, Hughen KA, Kaiser KF, Kromer B, McCormac FG, Manning SW, Reimer RW, Richards DA, Southon JR, Talamo S, Turney CSM, van der Plicht J, Weyhenmeyer CE (2009) IntCal09 and marine09 radiocarbon age calibration curves, 0–50,000 years cal BP. Radiocarbon 51:1111–1150

Shen J, Liu X, Wang S, Matsumoto R (2005) Palaeoclimatic changes in the Qinghai Lake area during the last 18,000 years. Quat Int 136:131–140

Tracey B, Lee N, Card V (1996) Sediment indicators of meromixis: comparison of laminations, diatoms, and sediment chemistry in Brownie Lake, Minneapolis, USA. J Paleolimnol 15:129–132

Wang J, Zhu L, Daut G, Ju J, Lin X, Wang Y, Zhen X (2009) Investigation of bathymetry and water quality of Lake Nam Co, the largest lake on the central Tibetan Plateau, China. Limnology 10:149–158

Wang Y, Liu X, Herzschuh U (2010a) Asynchronous evolution of the Indian and East Asian Summer Monsoon indicated by Holocene moisture patterns in monsoonal central Asia. Earth Sci Rev 103:135–153

Wang J, Zhu L, Wang Y, Ju J, Xie M, Daut G (2010b) Comparisons between the chemical compositions of lake water, inflowing river water, and lake sediment in Nam Co, central Tibetan Plateau, China and their controlling mechanisms. J Great Lakes Res 36:587–595

Wischnewski J, Mischke S, Wang Y, Herzschuh U (2011) Reconstructing climate variability on the northeastern Tibetan Plateau since the last Lateglacial—a multi-proxy, dual-site approach comparing terrestrial and aquatic signals. Quat Sci Rev 30:82–97

Wrozyna C, Frenzel P, Xie M, Zhu L, Schwalb A (2009) A taxonomical and ecological overview of recent and Holocene ostracods of the Nam Co region, southern Tibet. Quat Sci 29:665–677

Wu Y, Lücke A, Jin Z, Wang S, Schleser GH, Battarbee RW, Xia W (2006) Holocene climate development on the central Tibetan Plateau: a sedimentary record from Cuoe Lake. Palaeogeogr Palaeoclimatol Palaeoecol 234:328–340

Xu H, Liu B, Wu F (2010) Spatial and temporal variations of Rb/Sr ratios of the bulk surface sediments in Lake Qinghai. Geochem Trans 11:3

You Q, Kang S, Li C, Li M, Liu J (2006) Features of meteorological parameters at Nam Co station, Tibetan Plateau. Annual report of Nam Co monitoring and research station for multisphere interactions 1:1–8 (In Chinese with English abstract)

Zhang Q, Kang S, Wang F, Li C, Xu Y (2008) Major ion geochemistry of Nam Co Lake and its sources, Tibetan Plateau. Aquat Geochem 14:321–336

Zhang J, Chen F, Holmes JA, Li H, Guo X, Wang J, Li S, Lü Y, Zhao Y, Qiang M (2011) Holocene monsoon climate documented by oxygen and carbon isotopes from lake sediments and peat bogs in China: a review and synthesis. Quat Sci Rev 30:1973–1987

Zhu L, Wu Y, Wang J, Lin X, Ju J, Xie M, Li M, Mäusbacher R, Schwalb A, Daut G (2008) Environmental changes since 8.4 ka reflected in the lacustrine core sediments from Nam Co, central Tibetan Plateau, China. The Holocene 18:831–839

Zhu L, Zhen X, Wang J, Lü H, Xie M, Kitagawa H, Possnert G (2009) A ~30,000-year record of environmental changes inferred from Lake Chen Co, southern Tibet. J Paleolimnol 42:343–358

Zhu L, Peng P, Xie M, Wang J, Frenzel P, Wrozyna C, Schwalb A (2010a) Ostracod-based environmental reconstruction over the last 8,400 years of Nam Co Lake on the Tibetan plateau. Hydrobiologia 648:157–174

Zhu L, Xie M, Wu Y (2010b) Quantitative analysis of lake area variations and the influence factors from 1971 to 2004 in the Nam Co basin of the Tibetan Plateau. Chin Sci Bull 55:1294–1303